SESSION 1.

MAIN SEQUENCE AND SUPERGIANT STARS - I.

https://doi.org/10.1017/S0074180900148594 Published online by Cambridge University Press

Intrinsic Parameters of Hot Blue Stars

R.P. Kudritzki and D.G. Hummer*

Institut für Astronomie und Astrophysik der Universität München

*Staff Member, Quantum Physics Division, National Bureau of Standards; permanent address, Joint Institute for Laboratory Astrophysics, University of Colorado and National Bureau of Standards, Boulder, Colorado

I. Introduction

Advances in both theoretical understanding and observational capabilities in the past few years have made possible the determination of the effective temperature, surface gravity and chemical abundance of massive stars with unprecedented accuracy. These data are in turn important for the study of galaxies, as stars are important sources of information concerning the evolutionary state, past and present chemical composition, and distance of the parent galaxy. In addition to this diagnostic role, stars are crucial as sources of light, matter, and metals in the galaxy. Thus an improved understanding of massive stars makes possible a better determination of the physical conditions in a galaxy as well as a deeper understanding of how it functions.

The hottest stars in a galaxy fall into two distinct groups: 1) the young, massive, very luminous stars at the upper end of the main sequence with masses in the range 20-200 $M_\odot$; 2) the hot evolved stars with smaller masses and luminosities. Members of the first group, newly formed from the ISM, reflect the chemical composition of the galactic gas and provide information about the process of star formation. Their rapid evolution with strong mass loss, leading to Wolf-Rayet stars and Type II Supernovae, means that these stars in their various phases are responsible for the abundance of heavy elements in the galaxy. Because of their high luminosity, the stars can also be used as standard candles; a proposal for their exploitation in a new way appears at the end of this review.

The second group includes subdwarf O-stars, subdwarf B-stars and Extended Horizontal Branch objects, and central stars of planetary nebulae. These diverse objects have masses in the range 0.3 to 3 $M_\odot$ and are all in advanced stages of stellar evolution. As successors of the asymptotic giant branch, they exhibit abundance anomalies reflecting their evolutionary history rather than the composition of the ISM and so give less information on the current chemical content of the galaxy. On the other hand, as progenitors of White Dwarfs and probably of Type

C. W. H. De Loore et al. (eds.), Luminous Stars and Associations in Galaxies, 3–18.

I Supernovae, they play other roles in the development of galaxies. For brevity we will discuss only the first group; for the second group we refer to Kudritzki (1985).

II. The Photosphere of Hot Stars

The determination of stellar parameters from spectra requires a detailed understanding of the stellar photospheres (and in some cases of stellar winds), which is complicated by a severe failure of the classical assumptions of Local Thermodynamic Equilibrium (LTE). This has been suspected for many years and was clearly demonstrated by Peterson and Scholz (1971) who showed that the LTE absorption profiles of H I, He I and He II were much too weak. The reason is clear: because of the intense radiation field the radiative transitions occur much more rapidly than electron collisions. Consequently the rate equations for the level populations and the state of ionization are dominated by radiative processes, which are determined by solutions of the radiative transfer equations. As these involve the excitation and ionization state of the gas, the calculation of non-LTE model stellar atmospheres awaited the development of powerful numerical algorithms, which were first provided by Auer and Mihalas (1972, 1973). Detailed calculations by these workers and by Kudritzki (1973, 1976, 1979) showed that non-LTE absorption profiles are much stronger, leading to improved agreement with observation. The resulting relation between stellar parameters and the model profiles of the classification lines provided a new calibration of spectral types as a function of effective temperatures in the hands of Conti and co-workers (Conti and Alschuler, 1971; Conti, 1973; Conti and Frost, 1977).

However, for ζ Pup, the brightest O-star in the sky, attempts to determine the effective temperature by different methods led to serious discrepancies. The ratio of equivalent widths of He I and He II led to a spectral type O4, corresponding to $T_{eff} \approx 50000$ K (Baschek and Scholz, 1971; Conti, 1973; Conti and Frost, 1977). On the other hand, $T_{eff} \approx 35000$ K was inferred from the angular diameter, given by interferometry, together with the visual flux (Hanbury Brown, 1974; Code et al., 1976; Davis et al., 1970), and also from fits of the continuum energy distribution in the visual and UV to model atmosphere fluxes (Holm and Cassinelli, 1977; Underhill et al., 1979; Remie and Lamers, 1982). This outstanding descrepancy cast doubt on the adequacy of the theory of model atmospheres, which was based on the so-called "classical" assumptions: hydrostatic and radiative equilibrium, plane-parallel geometry and no blanketing by metal lines. In order to resolve this serious discrepancy a detailed analysis using NLTE model atmospheres and specially-obtained high-quality photographic spectra of ζ Pup was carried out by Kudritzki et al. (1983), who compared calculations with observed profiles of Balmer and Pickering lines and equivalent width of He I λ 4471. The crucial point in their method is that T_{eff}, log g and the helium abundance (y=He/(H+He) by numbers) are determined simultaneously by constructing fit curves in the (log g, log T_{eff})-plane, along which the calculated and observed equivalent

https://doi.org/10.1017/S0074180900148594 Published online by Cambridge University Press

widths agree (see Fig. 1). In this way Kudritzki et al. (1983) determined for ζ Pup the parameters T_{eff} = 42000 K ± 2500 K, log g = 3.5 ± 0.15 and y = He/(H+He) = 0.14 ± 0.02. The calculated energy distribution for these parameters agrees satisfactorily with the UV measures of Brune et al. (1979), Code and Meade (1979), and Jamar et al. (1976), and with the visual data of Johnson and Mitchell (1975), although the differences among the UV observations and uncertainties in the (small) values of E_{B-V} precludes an exact comparison.

How can this wide range of temperatures be understood? In the first place, the usual calibration of spectral types vs. T_{eff} assumes that the ratio of equivalent width of HeI λ 4471 Å and HeII λ 4542 Å is primarily a function of temperature, whereas the models of Kudritzki et al. (1983) show that this ratio became very sensitive to gravity for smaller values of log g than were previously used in model calculations (see Fig. 2). Recent discussions by Tobin (1983) and by Abbott and Hummer (1985) show that methods using measured angular diameters and flux distributions for stars with T_{eff} > 40000 K are intrinsically subject to large errors; the latter authors and Kudritzki et al. (1983) stress also that the strong dependence of the flux on gravity leads to very large uncertainties in temperatures, since the gravity is undetermined. Methods relying on the energy

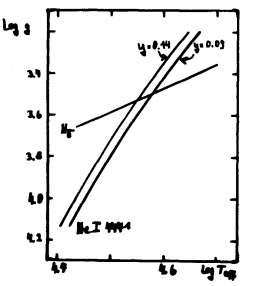

Fig. 1a. Fit diagram of Hγ and HeI λ 4471 for normal helium abundance y=0.09 and the enhanced value y= 0.14

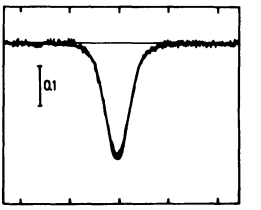

Fig. 1b. Hγ profile compared with calculation at the intersection point (y=0.14) in Fig. 1a

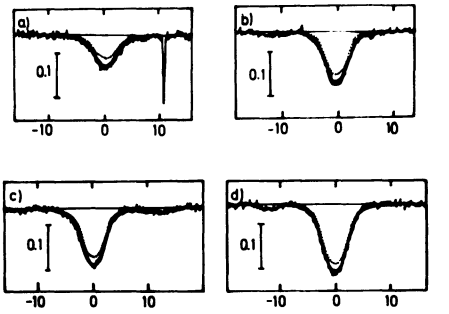

Fig. 1c. Profiles of He II lines compared with calculations at the intersections in Fig. 1a (dotted: y=0.09, full drawn: y=0.14)

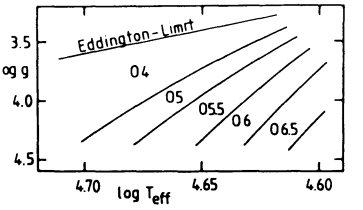

Fig. 2. The regions of the spectral types 04 to 06.5 in the log g-log T_{eff} diagram from NLTE models. The boundaries are given by W_λ(HeI4471)/W_λ(HeII4542) = 0.25, 0.35, 0.50, 0.63 and 0.79 from left to right.

https://doi.org/10.1017/S0074180900148594 Published online by Cambridge University Press

distribution alone are even worse. In practice the determination of T_{eff} from the continuous energy distribution is further compromised by the uncertainties in de-reddening the spectrum.

A further check on the accuracy of the derived model comes from a comparison of the interferometrically measured angular diameter (allowing for the electron scattering envelope) of $(4.1 \pm 0.3) \times 10^{-4}$ arc sec with that obtained by comparing the measured and computed fluxes, $(3.8 \pm 0.3) \times 10^{-4}$ arc sec. Finally the He II lines in the UV agree well with Copernicus spectra except for He II λ 1640 Å which, along with the visual line He II λ 4686 Å, can be shown to be formed in the wind.

We believe that the critical case of ζ Pup shows clearly that the method of non-LTE analysis of the line spectrum gives reliable values for T_{eff}, log g and y. Additional physical processes must be taken into account to realize the full accuracy of the method. This is discussed in the following two sections.

III. Wind Blanketing

Photons scattered by a stellar wind back into the photosphere heat the surface layers and modify significantly the observed spectrum, as was first discussed by Hummer (1982), who pointed out that for this purpose the wind could be represented by a partial reflector with an albedo depending on frequency, and who estimated the strength of the effect based on analytical solutions of gray atmospheres. Observational evidence for wind blanketing was presented by Remie and Lamers (1982). Husfeld (1982) and Husfeld and Kudritzki (1983) used schematic albedos with full non-LTE atmosphere models. The calculations by Abbott and Lucy (1985) of a realistic albedo for ζ Pup by a Monte-Carlo solution of the transfer problem in the wind accounting for approximately 10^4 lines

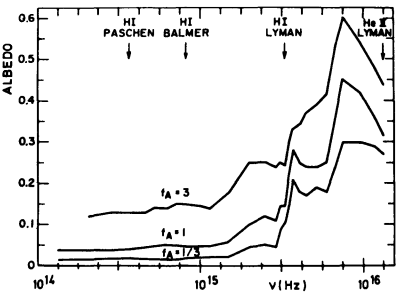

Fig. 3: Albedo vs. frequency for three values of mass loss rate. f_A is mass loss relative to that for ζ Pup ($\dot{M} = 5 \times 10^{-6} M_\odot$/yr)

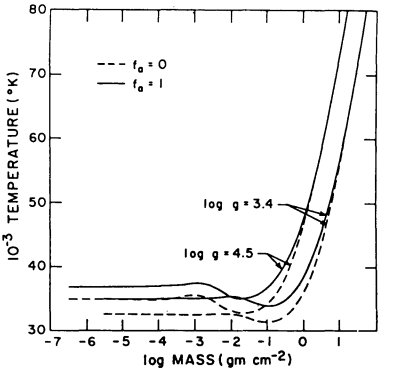

Fig. 4: Temperature vs. mass for T_{eff}=42000 K, log g=3.5. Curves are labeled with mass loss rate in units of that for ζ Pup

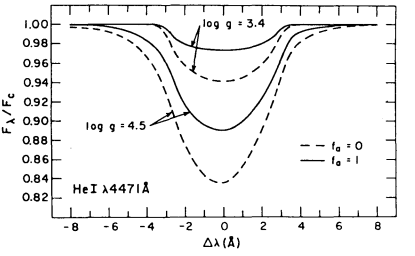

Fig. 5: Rotationally broadened line profile for He I 4471 Å, for models in Fig. 4

https://doi.org/10.1017/S0074180900148594 Published online by Cambridge University Press

made possible the calculations by Abbot and Hummer (1985) of non-LTE models with realistic wind blanketing. In Figure 3 the albedo is given for three cases, labelled with $f_A = \dot{M}/\dot{M}(\zeta\ \mathrm{Pup})$. Figure 4 shows the run of temperature in models for which T_{eff} = 42000 K, log g = 3.5, y = 0.16, for the indicated mass loss rates; the surface temperature for f_A = 1 is about 2000 K above the unblanketed model and that for f_A = 3, about 6000 K higher.

The classification lines for early-type O-stars are also affected by wind blanketing, particularly He I λ 4471 Å, as can be seen from Fig. 5 for the models of Fig. 3. Thus the spectral type depends not only on T_{eff} and log g, but also on the mass loss rate $\dot{M}$! An analysis by Bohannan et al. (1985) of line profiles of ζ Pup, obtained with a CCD camera, in which the full profiles of a large number of H, He I and He II lines were fit by wind-blanketed models, yields T_{eff} = 41500 K ± 1500, log g = 3.5 ± 0.1 and y 0.17 ± 0.03. An analysis of the same data using unblanketed models gave a value of T_{eff} larger by some 4000 K! The agreement between the parameters obtained by Bohannan et al. from wind-blanketed models and those of Kudritzki et al. (1983) from unblanketed models is fortuitous and arises from a systematic difference between He I λ 4471 Å measures in the two sets of observations.

IV. Metal opacity and non-LTE line blanketing.

Nearly all of the non-LTE models at present in use contain only H and He; the atmospheric structure from these models is used to calculate the line profiles for metals in order to determine abundances, but the effects of the metals on the structure is usually neglected. One exception is the grid of models calculated by Mihalas (1972), which contain a "mean light ion" intended to simulate the continuum opacity of the ground states of C, N, O and their ions. Husfeld et al. (1984) included more detailed C, N and O opacities and concluded that these opacities were of minor importance to the atmospheric structure.

Another effect of great potential significance for the photospheres of hot stars is the blocking of outflowing radiation by a large number of lines, particularly in the UV. Although the calculation of line-blanketed models for cooler stars in which LTE is a valid assumption has been brought to a remarkable degree of elaboration, principally by Kurucz (1979), the correct treatment for hot stars requires a full non-LTE treatment of hundreds or even thousands of lines. Anderson (1985) has developed an ingenious procedure for carrying out these calculations efficiently. To date Anderson has been able to include all H and He lines and the most important lines and continua of C and its ions, as well as the bound-free transitons of N, O, Ne, Mg, Si and S, in a model with T_{eff} = 35000 K and log g = 4.0. The surface temperature is controlled by the resonance doublet of C λλ 1548 Å, which cools the gas from about 28500 K in an unblanketed H-He model to about 17300 K. However, from the region of the temperature minimum of the corresponding H-He model inwards the temperature is essentially unchanged, i.e.

https://doi.org/10.1017/S0074180900148594 Published online by Cambridge University Press

no back warming is seen, contrary to what might have been expected. The combined effects of wind-blanketing, which heats the surface layers, and line-blanketing, which causes them to cool, are not yet known. As the heat capacity of the very low density gas at the top of a classical photosphere is so low, a small increase in the radiation field can cause a substantial change in temperature. Moreover, it seems plausible that the C IV resonance line in the wind may seriously reduce the ability of this transition to cool the photosphere.

The spectrum in the visual and UV regions including the lines of H I, He I and He II differs little from that of a standard non-LTE H-He model, but the flux at the confluence of the Lyman series, shortwards of approximately λ 921 Å, lies an order of magnitude below the standard model. Shortwards of the Lyman limit there are more significant discrepancies.

V. Radiation-driven Winds

There is now quite strong evidence that stellar winds in hot stars are driven by the force of radiation streaming from the photosphere, primarily through its interaction with the spectral lines, and that this phenomena is described, in its overall behaviour, by an improved version of the theory of Castor, Abbott and Klein (1975; =CAK), based on an earlier form of Lucy and Solomon (1970). Although controversy on this subject continues, very little in the way of quantitative production has been forthcoming from alternative theories.

A major step forward was taken by Abbott (1982), who calculated the radiative force using a list of approximately 10^4 lines. Although the physical representation of the line force was by far more realistic than with the original CAK line force, significant descrepancies still remained. In particular, $\dot{M}$ was systematically too large for OB-stars by a factor of 2-3 and too low for Wolf-Rayet stars by an order of magnitude, while the terminal velocity v_∞ was predicted to be roughly 1.3 v_{esc} instead of the observed value of 2-4.

A number of recent further improvements to the theory have led to significantly better agreement with observation. Pauldrach, Puls and Kudritzki (1986) have introduced into the CAK theory a factor accounting for the finite diameter of the photospheric disk, which results in much larger values of v_∞, in substantial agreement with observations. (This effect was also considered by Friend (1982)). These authors also solved the radiative transfer and gas dynamical equations using a sample of lines from Abbott's list, with strong, intermediate and weak lines weighted to reproduce Abbott's line force. This calculation is similiar to that of Weber (1981) but with technical and physical improvements. The agreement of v_∞ from the two methods, and with observation is remarkable, and in most cases the value of $\dot{M}$ also agrees with observations as can be seen in the following table.

https://doi.org/10.1017/S0074180900148594 Published online by Cambridge University Press

Comparison of observed and theoretical wind properties

star	Sp.Type	10^{-4} T_{eff}	log g	$R/R_\odot$	$\dot{M}$ (obs)	$\dot{M}$ (MCAK)	$\dot{M}$ (CMF)	v_∞ (obs)	v_∞ (MCAK)	v_∞ (CMF)
					$10^{-6} M_\odot$/yr			km/sec		
P Cyg	B1Ia	1.8	2.0	68	20.	29.	23.	400	395	355
ε Ori	B0Ia	2.9	3.3	37	3.1	3.3	2.6	2010	1950	2055
ζ Ori	O9.5I	3.0	3.4	29	2.3	1.9	-	2290	2274	-
ρ Sgr	O4(f)V	5.0	4.1	12	4.0	4.0	3.8	3440	3480	3860
HD48099	O6.5V	3.9	4.0	11	0.63	0.64	-	3500	3540	-
HD42088	O6.5V	4.0	4.1	6.2	0.13	0.20	0.20	2600	2600	2720
λ Cep	O6ef	4.2	3.7	17	4.0	5.1	4.3	2500	2500	2590

MCAK = Modified CAK, CMF = Co-Moving Frame (solution of transport and dynamical equations)

This theory, used with correctly determined atmospheric parameters for the Wolf-Rayet star V-444 Cygni including an effective temperature of approximately 90000 K (Cherepashchuk, Eaton and Khaliullin, 1984), reproduces not only the observed mass loss and terminal velocity, but also the run of velocity and density in the W-R wind as inferred by Cherepashchuk et al. from multi-colour light curves (Pauldrach, Puls, Hummer and Kudritzki, 1985).

Another important result of this work is that v_∞/v_{esc} is not a constant but a function of g, T_{eff} and R. Consequently its mass loss rate will not be a unique function of the location in the H-R diagram, but will also depend on the evolutionary state of the star. This circumstance seems not to have been appreciated by critics of the radiation-driven wind theory. We believe that the time-averaged stationary wind properties of hot stars can be explained by this theory.

The direct numerical solution of the coupled radiation-gas dynamical equations allows the calculation of line force to be carried out in the subsonic region of the flow where the Sobolev approximation is unreliable. Thus the properties of the radiation-driven flow can be followed down into the photosphere. It turns out that the radiation pressure in the lines, which is usually neglected in calculating the photospheric radiation pressure, may be comparable to the usual continuum contribution for low gravity objects. Therefore the value of log g inferred by fitting to line profiles will be too small; for low gravity objects the effect will be on the order of 0.15 dex (Pauldrach, Puls and Kudritzki, 1986). Such calculations also provide the basis for a realistic calculation of extended photospheres, as appropriate to both high-luminosity O-B stars as well as to certain nuclei of planetary nebulae. Extended spherical model atmospheres with density distribution obtained in this way are now being developed in Munich.

https://doi.org/10.1017/S0074180900148594 Published online by Cambridge University Press

VI. The H-R Diagram of the Most Massive Galactic O-Stars

The techniques described in section II for ζ Pup have been applied to the galactic 03-stars in the η Car region (Kudritzki, 1980; Simon et al., 1983). The results are given in the following table.

Parameters of the most luminous galactic O-stars

star	spectral type	T_{eff} 10^3 K	log g (cgs)	y	log $L/L_\odot$	M_V
HD 93250	03V((f))	52	3.95	0.09	6.3±0.1	-6.4±0.25
93128	"	48	3.85	0.09	5.7±0.1	-5.2±0.25
303308	"	45	3.90	0.09	5.8±0.1	-5.5±0.25
93129A	03If	45	3.60	0.09	6.2±0.1	-6.6±0.25
ζ Pup	04f	42	3.50	0.14	6.0±0.4	-6.0±1.00

The accuracy for T_{eff}, log g and y is ±3000 K, ±0.15 and ±0.02, respectively. It is obvious from the table that most of the 03 stars are significantly cooler than the previously assumed value of 53000 K assigned to all 03 stars by Conti and Burnichon (1975). Moreover, they reveal a large spread in effective temperature, absolute magnitude and luminosity, which means that the detailed spectroscopic analysis technique as described above is needed to construct a reliable HR-diagram for these very luminous blue objects.

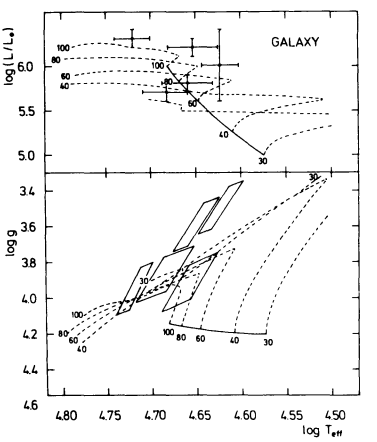

Fig. 6: (see text)

The loci of these five objects in the (log g, log T_{eff}) and (log L, log T_{eff}) forms of the H-R diagram are given in Figure 6, along with the newly calculated evolutionary tracks of Pylyser, Doom and de Loore (1985), which include the effects of mass loss, adjusted to yield the Humphreys-Davidson limit, and of overshooting according to the Roxburgh (1978) criterion. As the transformation between the two diagrams is trivial for the theoretical tracks, because the mass at each point is known, while that for the observed stars involves photometric and distance information, this way of comparing theory with observations gives more information than either form of the H-R diagram alone. In the first place, if the locus of a par-

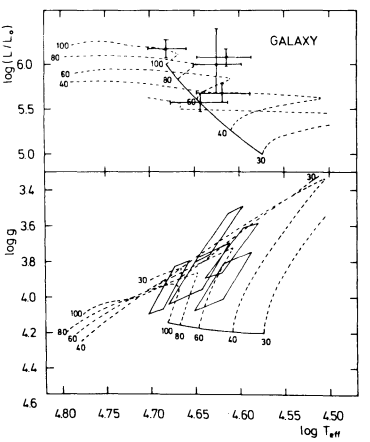

Fig. 7: (see text)

https://doi.org/10.1017/S0074180900148594 Published online by Cambridge University Press

ticular star does not have a consistent relation to the track of a given mass, one is alerted to the certainty of error. Moreover the luminosity form gives better mass discrimination, while the log g form allows for a more direct test of evolution theory (but only if T_{eff} and log g are determined with sufficient precision).

In the present case we see that HD 93128 looks somewhat suspicious, although the extremes of the error bars include the same mass tracks. Also the two low-gravity stars HD 93129A and ζ Pup seem to lie outside the region of the tracks. It is therefore of interest to note the consequences of two effects discussed above (sections IV and V) which have not yet been included in the determination of these parameters: 1) wind blanketing can be expected to reduce T_{eff} by 4000-5000 K (except for ζ Pup) and 2) the effect of line radiation pressure in the photosphere can be expected to increase log g of the two low-gravity stars by approximately 0.15 dex. Thus the error boxes of these two stars will be expected to move down in the (log g, log T_{eff})-plane by 0.15 dex and the loci of all stars (except ζ Pup) will be shifted to the right by approximately .04 dex, as shown in Fig. 7. We stress that these changes are not based on detailed calculations for the individual objects. The agreement of the photometrically determined masses with the track masses seems to be considerably better in Fig. 7.

It is interesting that ζ Pup has both the largest luminosity and an enhanced helium content, indicating that it is substantially further evolved than the other four stars. Butler and Simon (1985) find in a preliminary analysis that its N abundance is enhanced by a factor between 6 and 10.

VII. Abundances in Massive O-stars

Non-LTE abundance determinations are based on statistical equilibrium calculations for the element in question using the appropriate model atmosphere to provide the run of temperatures, density and radiation field. Rotational broadening and collison broadening enter at this stage. The demands for atomic radiative and collisional data are enormous and frequently rather unreliable data must be used. Detailed abundance analyses have been made in this way by many workers, which cannot be reviewed here for lack of space. However, very recently Schönberner, Kudritzki and Simon (1984, 1985) have carried out an abundance study of He, C, N, O in 7 O-stars. Four of these objects are socalled "ON-stars", as their spectra show abnormally strong lines of nitrogen (Walborn, 1970, 1971, 1976). The other three objects are normal O-stars, which are used as standards for a differential study of the abundance of the strategic CNO-elements as an important prerequisite for a discussion of the evolutionary history of ON-stars.

The abundance analysis proceeds in two steps. First, the atmospheric parameters (T_{eff}, log g, y) are determined by the same techniques described in section II. This leads to a very interesting result which is displayed in the following table:

https://doi.org/10.1017/S0074180900148594 Published online by Cambridge University Press

Atmospheric parameters

normal stars				ON-stars			
name	10^{-3} T_{eff}	log g (cgs)	y	name	10^{-3} T_{eff}	log g (cgs)	y
τ Sco	33	4.15	0.1	HD 89137	30.0	3.25	0.26
10 Lac	38	4.25	0.09	Car	32.5	4.15	0.17
15 Mon	41	4.1	0.08	HD 14633	35.5	3.70	0.15
				HD 48279	37.5	4.00	0.15

Strikingly, all ON-stars are helium enriched, whereas the normal stars have normal helium abundance! The helium enrichment is strongest for HD 89137, which as a low gravity object has evolved away from the ZAMS.

An obvious question is whether the helium enrichment is due to the CNO-cycle. This is investigated in the second step where the C,N,O-lines (optical and UV high resolution spectra) are analysed on the basis of final non-LTE models and line-formation calculations (the latter carried out totally in a NLTE multi-level form for N III, but in LTE for the other ions). The results are given in the table:

CNO-Abundance of O and ON-stars

normal stars						ON-stars					
object	C	N	O	N/C	N/O	object	C	N	O	N/C	N/O
τ Sco	-3.9*	-3.9	-2.9	1.0	0.2	HD 89137	-4.2	-2.3	-2.9	80	4
10 Lac	-3.2	-3.9	-2.7	0.2	0.06	θ Car	-4.7	-2.9	-3.1	65	1.5
15 Mon	-3.1	-4.0	-	0.1	-	HD 14633	-4.5	-2.7	-3.1	60	2.5
Sun	-3.36	-4.04	-3.12	0.2	0.1	HD 48279	-4.1	-2.6	-2.7	30	1.0

* columns C, N and O contain log ε, where ε is the number fraction: $\varepsilon = n_x / \Sigma\, n_x$

The abundances of the normal stars are essentially solar (except for carbon in τ Tau, which is well known already (Hardorp and Scholz, 1970)). However, for the ON-stars nitrogen is strongly enriched, carbon is strongly depleted and O remains about solar. This allows one to draw the firm conclusion that these stars are exposing nuclear processed matter at their surfaces. The elemental distribution corresponds to that of the incomplete CNO-cycle, where only the CN-equilibrium is well established (see Fig. 8). Fig. 9 shows the (log g, log T_{eff})-

https://doi.org/10.1017/S0074180900148594 Published online by Cambridge University Press

diagram of the objects compared with evolutionary tracks by Maeder, 1982, which include convective mixing, overshooting and mass-loss. Qualitatively, the idea of photospheric enrichment by nuclear processed material as evolution proceeds is supported by Fig. 9. However, quantitativley the abundances are not in agreement. It is also not clear why the two ON-stars close to the ZAMS show CN-burned material. As they are binaries, the turbulent mixing due to shear instabilities is perhaps more efficient in carrying CN-burned matter to the surface.

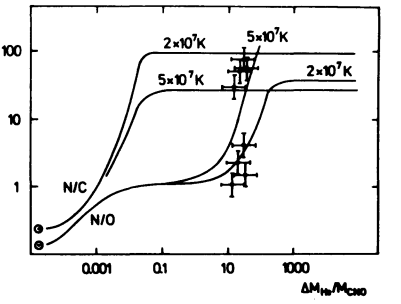

Fig. 8. Theoretical ratios of N/C and N/O as a function of newly created helium per total CNO-abundance (according to Caughlan, 1965). The observed ratios for the ON-stars are also plotted.

VIII. Abundance Gradients in the Galactic Disk from Young Cluster B-stars

Observed abundance distributions in the disk set important constraints on theories of galactic evolution (Güsten and Mezger, 1983) and the abundance ratios (especially isotopic ratios) contain in principle information on the production processes (Talbot and Arnett, 1973). Analyses of emission lines of planetary nebulae and H II regions have yielded logarithmic abundance gradients of the order of -0.05 dex/kpc for N and O. Very recently this question has been investigated by Gehren et al. (1985), who determined the N and O abundances of a large sample of young B-stars in open clusters lying in the Galactic disk. As these stars are very young their abundances represent those of the gas from which they were formed. Moreover they are well described by stellar models, since convection is negligible and deviations from LTE are small. Using the Cassegrain echelle spectrograph (CASPEC) with a CCD detector on the ESO 3.6 m, high-resolution spectra have been obtained for remote open clusters, covering a range of galactocentric distances from 8.5 to 19.5 kpc.

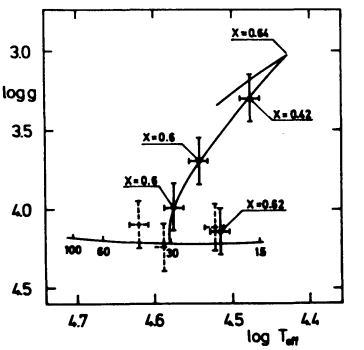

Fig. 9. The (log g, log T_{eff})-diagram of ON-stars (full drawn crosses) and normal O-star standard (dashed crosses). Evolutionary tracks by Maeder (1982) are also shown. For the ON-stars the hydrogen mass-fraction is indicated.

A preliminary analysis of this material has been carried out using LTE model atmospheres, which should be adequate for a differential analysis in view of the low effective temperatures of these stars (T_{eff} < 30000 K). A grid of LTE models with solar He/H and metal/H abundances was calculated allowing for the Balmer and Lyman series as well as the

https://doi.org/10.1017/S0074180900148594 Published online by Cambridge University Press

100 strongest metal lines. The resulting temperature stratifications were nearly identical with those obtained by Kurucz (1979). T_{eff} and log g were determined from fits to Hβ and Hγ line profiles and from the relative strengths of Si II, Si III and Si IV lines. For each star 25 N II and 120 O II lines were used to determine the abundances. All abundances were determined relative to the standard star BS 2928, for which the abundances relative to the sun were found by Lambert (1978). This approach minimizes systematic errors arising from uncertain oscillator strengths and line broadening parameters, as well as small non-LTE effects (which may affect the sample as a whole). Figure 10 shows the abundance ratios N/H, O/H and N/O as functions of galactocentric distance. These results are consistent with a conclusion that no significant abundance gradient exists in the outer part of the Galaxy. Moreover, the scatter of roughly a factor of 2 in abundances for a given cluster is real.

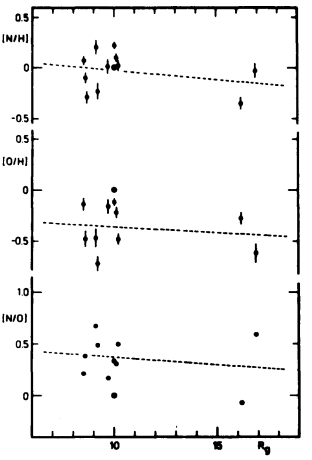

Fig. 10: Logarithmic N and O abundances and N/O ratios vs. galctocentric distance R_g. 2σ error bars refer to rms. error of single stars and include systematic errors. Dashed lines are least square fits.

IX. Future Developments

In addition to the recent developments in the theory of stellar atmospheres and winds described above, a very important contribution is now being made by the London-Belfast-Boulder opacity project, which is producing photoionization cross sections, oscillator strengths, damping coefficients and electron scattering cross sections of unprecedented accuracy and completeness for all atoms and ions of astrophysical interest.

These developments are matched by dramatic improvements in observational techniques. Capabilities for UV and IR spectroscopy continue to increase by leaps and bounds. Modern spectrographs and solid state detectors of high quantum efficiency and (hopefully) linear response make possible the spectroscopy of a wide range of stars, with characteristics summarized in the following Table:

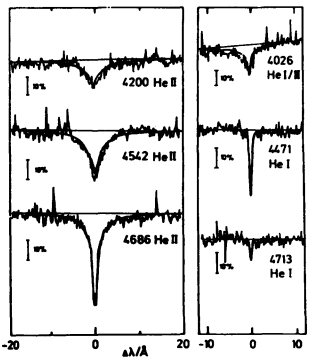

Fig. 11: He I and He II lines of ROB 162, and profiles calculated from final models.

https://doi.org/10.1017/S0074180900148594 Published online by Cambridge University Press

m_v	S/N	$\Delta\lambda/\lambda$	t_{exp}
$\leq 7^m$	100-1000	10^4-10^5	< 60 min
7^m-14^m	30-100	2×10^9	< 90 min
14^m-20^m	10-50	2×10^3	120 min

Consequently accurate quantitative spectroscopy on very distant as well as nearby stars is now feasible. Thus we can investigate in detail the evolution of stars in all stages, which in turn allows us to study the structure and chemical evolution of galaxies.

An example of recent work illustrates the current situation. Figure 11 shows the He lines of ROB162, the only hot sdO star (m_v = 13.3) in the metal-deficient globular cluster NGC 6397. These spectra, with S/N≈ 30 and $\lambda/\Delta\lambda \approx 2 \times 10^4$, were obtained with 60 minute exposures on the ESO 3.6 m using CASPEC with a CCD detector. Heber and Kudritzki (1984) have determined the parameters T_{eff} = 51000 K ± 2000 K, log g = 4.5 ± 0.2 and n_{He}/n_H = 0.1 ± 0.02; calculated profiles for models with these parameters are given in the Figure.

We and collaborators in Munich and Boulder have underway a long-term project studying the evolution of massive stars in the Galaxy and the Magellanic Clouds, using spectra obtained with CASPEC on the ESO 3.6 m. We plan to obtain UV spectra with the High Resolution Spectrograph when Space Telescope becomes available. By means of wind-blanketed model atmospheres we can analyze these spectra, as outlined above, to determine T_{eff}, log g, abundances and M for a large number of stars. Thus we will obtain reliable H-R diagrams as well as information on chemical abundances and their spatial distributions for three galaxies of substantially different metallicities. These data provide meaningful constraints on many aspects of stellar evolution theory: main sequence location and width, the evolution of massive stars, the effects of mass loss and turbulent mixing, CNO-production and the evolution to WR stars and Type I Supernovae, all as functions of galactic metallicity. Moreover various aspects of chemical evolution, such as abundance gradients and IMF, can be studied as functions of Z. We are also interested in the role of hot stars as sources of ionization of H II regions: are the properties and abundances of ionized regions consistent with those of the ionizing stars? A first step in this program is reported by Gehren et al. (1986).

A further, and possibly more far reaching, application of the developments can now be considered - the use of massive stars as distance indicators. The idea is simple: by determining T_{eff} and log g from spectral lines by means of non-LTE model analysis and observing the terminal velocity v_∞, one has three relations among the three fundamental quantities mass, luminosity and radius. Specifically, from the relation between v_∞ and v_{esc} given above, and knowing v_∞, T_{eff} and g, one finds R and thus L or M_v. From a preliminary analysis, it appears

https://doi.org/10.1017/S0074180900148594 Published online by Cambridge University Press

that one can determine g to sufficient accuracy from observations of the Balmer lines with a FWHM resolution of < 3Å, or perhaps even 5Å if good S/N can be obtained. High accuracy in T_{eff} is not needed. For faint objects, Space Telescope will make possible the observations of UV lines to find v_∞.

We can see how well this idea works by using it on four of the five stars discussed in Section VI for which v_∞ is known from IUE observations. These data are summarized in the following table:

Star	v_∞	$r/R_\odot$	M_V (derived)	M_V (literature)
HD 93250	3300 km/s	19	-6.5	-6.4
93129	3950	27	-7.1	-6.6
303308	3200	14	-5.7	-5.5
ζ Pup	2400	19.5	-6.3	-6.0

These results encourage us to believe that we can provide new information on distances of galactic OB stars and central stars of planetary nebulae. Can this purely spectroscopic method be used for extragalactic objects? As an example, consider Space Telescope with the Faint Object Camera or Faint Object Spectrograph, using the long slit. With $\lambda/\Delta\lambda \approx$ 1000-2000, the limiting magnitude is $m_v \approx 23$ for both blue and V spectral regions. Thus with $M_V \approx -6$, we have $m-M_V \approx 29^m$.

D.G. Hummer acknowledges a "Senior U.S. Scientist Award" from the Alexander von Humboldt Stiftung.

References

Abbott, D.C., 1982, Ap.J. 281, 774
Abbott, D.C. and Hummer, D.G., 1985, Ap.J., 294, 286
Abbott, D.C. and Lucy, L.B., 1985, Ap.J., 288, 679
Anderson, L.S., 1985, Ap.J., 15 Nov.
Auer, L.H and Mihalas, D., 1972, Ap.J.Suppl., 24, 153
Auer, L.H and Mihalas, D., 1973, Ap.J.Suppl., 25, 433
Baschek, B. and Scholz, M., 1971, Astron. Astrophys., 15, 285
Bohannan, B., Abbott, D.C, Voels, S.A. and Hummer, D.G., 1985, these Proceedings
Brune, W.H., Mount,G.H. and Feldman, P.D., 1979, Ap.J. 227, 884
Butler, K. and Simon, K.P., 1985, Proc. ESP Workshop on CNO Abundances, ed. I.J. Danziger
Castor, J.I., Abbott, D.C. and Klein, R.I., 1985, Ap.J. 195, 157
Cherepashchuk, A.M., Eaton, J.A. and Khaliullin, K.F., 1984, Ap.J. 281, 744
Code, A.D., Davis, J., Bless, R.C, and Hanbury Brown, R., 1970, MNRAS 189, 601
Code, A.D and Meade, M.R., 1979, Ap.J.Suppl. 39, 195
Conti, P.S., 1973, Ap.J. 179, 181
Conti, P.S. and Alschuler, W.R., 1971, Ap.J. 170, 325
Conti, P.S. and Frost, S.A., 1977, Ap.J. 212, 728

Davis, J., Morton, D.C., Allen, L.R., and Hanbury Brown, R., 1970, MNRAS 150, 45
Friend, D.B., 1972, Ph.D.Thesis, Univ. of Colorado
Gehren, T., Husfeld, D., Kudritzki, R.P., Conti, P.S. and Hummer, D.G., 19 6, these Proceedings
Gehren, T., Nissen, P.E., Kudritzki, R.P. and Butler, K., 1985, Proc. ESO Workshop on CNO Abundances, ed. J.J. Danziger
Güsten, R. and Mezger, P.G., 1983, Vistas in Astronomy 26, 159
Hanbury Brown, R., Davis, J. and Allen, L.R., 1974, MNRAS 167, 121
Hardorp, J. and Scholz, M., 1970, Ap.J.Suppl 19, 193
Heber, U. and Kudritzki, R.P., 1984, Mitt. Astron. Ges. 62, 249
Holm, A.V. and Cassinelli, J.P., 1977, Ap.J. 211, 432
Hummer, D.G., 1982, Ap.J. 257, 724
Husfeld, D., 1982, Diplomarbeit, Univ. Kiel
Husfeld, D. and Kudritzki, R.P., 1983, Mitt. Astron. Ges. 60, 306
Husfeld, D., Kudritzki, R.P., Simon, K.P. and Clegg, R.E.S., 1984, Astron. Astrophys. 134, 139
Jamar, C., Macau-Hercot, D., Monfils, A., Thompson, G.I., Hoziaux, L., and Wilson, R., 1976, Ultraviolet Bright-star Spectrophotometric Catalogue (ESA SR-27)
Johnson, H.L. and Mitchell, R.I., 1975, Rev. Mex. Astrf. Af. 1, Nr. 3
Kudritzki, R.P., 1973, Astron. Astrophys. 28, 103
Kudritzki, R.P., 1976, Astron. Astrophys. 52, 11
Kudritzki, R.P., 1979, Proc. of 22nd Liege conf., 295
Kudritzki, R.P., 1980, Astron. Astrophys. 85, 174
Kudritzki, R.P., 1985, Proc. ESO Workshop on CNO Abundances, ed. I.J. Danziger
Kudritzki, R.P., Simon, K.P. and Hamann, W.R., 1983, Astron. Astrophys. 118, 245
Kurucz, R., 1979, Ap.J.Suppl. 40, 1
Lambert, D.L., 1978, MNRAS 182, 249
Lucy, L.B. and Solomon, P., 1970, Ap.J. 159, 879
Maeder, A., 1982, Astron. Astrophys. 105, 149
Mihalas, D., 1972, Non-LTE Model Atmospheres for B and O Stars, NCAR-TN/STR-76, National Center for Atmospheric Research, Boulder
Pauldrach, A., Puls, J., Hummer, D.G. and Kudrizki, R.P., 1985, Astron. Astrophys. 148, L1
Pauldrach, A., Puls, J. and Kudritzki, R.P., 1986, Astron. Astrophys., to be submitted
Peterson, D.M. and Scholz, M., 1971, Ap.J. 163, 51
Pylyser,E., Doom, C. and de Loore, C., 1985, Astron. Astrophys., in press
Remie, H. and Lamers, H.J.G.L.M., 1982, Astron. Astrophys. 105, 85
Roxburgh, I.W., 1979, Astron. Astrophys. 65, 281
Schönberner, D., Kudritzki, R.P. and Simon, K.P., 1984, Proc. 4th Europ. IUE Conf., ESA SP-118, p. 267
Schönberner, D., Kudritzki, R.P. and Simon, K.P., 1985, Astron. Astrophys., to appear
Simon, K.P., Jonas, G., Kudritzki, R.P. and Rahe, J., 1983, Astron. Astropys. 125, 34
Talbot, R.J. and Arnett, W.D., 1973, Ap.J. 186, 51

Tobin, W., 1983, Astron. Astrophys. 125, 168
Underhill, A.B., Divan, L., Prevot-Burnichon, M.L., Doazan, V., 1979, MNRAS 189, 601
Walborn, N.R., 1970, Ap.J. 161, L149
Walborn, N.R., 1971, Ap.J. 164, L67
Walborn, N.R., 1976, Ap.J. 205, 419
Weber, S.V., 1981, Ap.J. 243, 954

Discussion : KUDRITZKI & HUMMER

SREENIVASAN :

I am happy to learn of the improvements you have made to stellar wind-theory. Have you also included a realistic energy conservation statement in the theory? CAK assumed radiative equilibrium and used a temperature profile in accordance with that assumption.

KUDRITZKI :

We have performed test calculations, which show that the temperature stratification in the wind is not crucial for the dynamics of the wind. We have used constant temperatures of different values as well as radiative equilibrium stratifications. That had nearly no effect on the mass loss rate as well as on V_{inf}.

LAMERS :

The observations show that the ratio V_{inf}/V_{esc} decreases with temperature from 3.5 at $T_{eff} \geq 30.000K$ to 1 at T_{eff} 10.000 K. This relation is important in your proposed methods for distance calibration. Do your calculations agree with this observed relation?

KUDRITZKI :

Yes, at least down to T_{eff} 20.000 K (P Cygni). We did not yet calculate winds for cooler stars like, for instance, alpha Cygni (T_{eff} 9000 K), where it is not clear whether our theory still works. The advantage of these cooler objects is that their absolute V-magnitude is brighter. However V_{inf} is propably too small to be measured with sufficient accuracy.

https://doi.org/10.1017/S0074180900148594 Published online by Cambridge University Press